GEOSTANDARDS and GEOANALYTICAL RESEARCH

Determination of the Isotopic Composition of an Enriched Hafnium Spike by MC-ICP-MS Using a Regression Model

Ran **Lin** (1, 2), Jie **Lin** (1), Keqing **Zong** (1, 2), Kang **Chen** (1), Shuoyun **Tong** (1), Lanping **Feng** (1), Wen **Zhang** (1), Ming **Li** (1), Yongsheng **Liu** (1, 2), Zhaochu **Hu** (1) and Lian **Zhou** (1)

(1) State Key Laboratory of Geological Processes and Mineral Resources, China University of Geosciences, Wuhan, 430074, China
(2) School of Earth Sciences, China University of Geosciences, Wuhan, 430074, China
* Corresponding author. e-mail: linjiecug@foxmail.com

The isotope dilution (ID) method, owing to its high precision, is extensively used for the determination of element mass fractions in a wide range of natural samples. One of the prerequisites of the ID method is knowledge of the isotopic composition of an enriched spike, which is often challenging to accurately determine. In this study, we employ a regression mass bias correction model to accurately and precisely measure the isotopic composition of an enriched Hf spike (Lot No. 159293, Oak Ridge National Laboratory). A NIST SRM 3134 Re solution, whose isotopic composition was calibrated by an NRC IRIS-1 Ir isotope standard, was used to calibrate the isotopic composition of the Hf spike. The obtained ratios of ^{176}Hf/^{177}Hf, ^{179}Hf/^{177}Hf and ^{180}Hf/^{177}Hf were 0.2406 ± 0.0005 (u, k = 1), 2.8620 ± 0.0005 (u, k = 1) and 384.65 ± 0.05 (u, k = 1), respectively, which meet the required precision levels for Hf isotopes in the application of the ID method. The combined uncertainties of the calibrated Re and Hf isotope ratios were evaluated using a Monte Carlo method, in which the uncertainty of the primary calibrator (IRIS-1, ^{193}Ir/^{191}Ir = 1.6866 ± 0.0005, u, k = 1) was also taken into consideration. The precision of Hf spike was improved significantly compared with the SSB and C-SSBIN methods. To the best of our knowledge, this is the first report of isotope ratio calibration in an enriched spike using the regression model. The precisely calibrated spike can lower the uncertainty of the Hf mass fraction significantly, thereby increasing the accuracy of the Lu-Hf chronometer.

Keywords: Hf isotopic composition, enriched spike, isotope dilution, regression model.

Received 19 Oct 19 – Accepted 23 Apr 20

Compared with the ^{40}K-^{40}Ar, ^{87}Rb-^{87}Sr and ^{238,235}U-^{206,207}Pb radiogenic isotopic systems, the ^{176}Lu-^{176}Hf system, with a half-life of ~ 37 billion years, is both a versatile geochronometer and a powerful tool for studying the processes that control crust–mantle evolution (Scherer *et al.* 2001). The ^{176}Lu-^{176}Hf system offers the advantage of retaining age information at a higher temperature than Sm-Nd, providing a potential opportunity to date garnet growth in crust and mantle environments (Scherer *et al.* 2000, Barfod *et al.* 2003) by exploiting Hf-poor inclusions in garnet, which yield higher ^{176}Hf/^{177}Hf and ^{176}Lu/^{177}Hf values suitable for Lu-Hf measurement (Patchett and Tatsumoto 1980a). Previously, routine Hf isotope measurement was prevented by the poor ionisation efficiency of Hf during thermal ionisation mass spectrometry (TIMS) (Blichert-Toft *et al.* 1997). However, with the development of multi-collector inductively coupled plasma mass spectrometry (MC-ICP-MS), the accuracy and precision of the measurement of Hf have now improved (Blichert-Toft 2001), and the ^{176}Lu-^{176}Hf system has become a significant geochronometer in geochemistry and cosmochemistry (Patchett and Tatsumoto 1980b, Lagos *et al.* 2007). In geochronology, isotope dilution (ID) was first applied to geology in the determination of microgram quantities of lead from rocks by Marshall in the 1960s (Marshall and Hess 1960) and it has been developed as one of the analytical methods that provide the most accurate and precise mass fraction values (Becker and Dietze 1998). In addition, ID can minimise uncertainties on the calculated ages of rocks, which critically depend on the uncertainties of the isotope ratio affected by the determined parent and daughter element mass fractions in the Sm-Nd (Smit *et al.*

doi: 10.1111/ggr.12343

2013, Shu *et al.* 2014), U-Th-Pb (Cheng *et al.* 2012) and Rb-Sr (Waight *et al.* 2002, Beranoaguirre *et al.* 2019) isotopic systems. Therefore, ID is becoming increasingly important to geochronology (Le Fèvre and Pin 2005, Brun *et al.* 2009, Willbold and Jochum 2010, Gopalan 2011, Herwartz *et al.* 2011). The ID method is based on the addition of a known quantity of spike to a known quantity of a sample by measuring the isotope ratio in the spike–sample mixture using mass spectrometry. One critical prerequisite of calculating the mass fraction of the analyte in the original sample is the accurate mass fraction and isotopic composition of the spike. For ideally spiked samples, the accuracy and precision of the sample isotope ratios and mass fractions determined by ID depend on a number of additional factors, but most of the uncertainty is from the uncertainty of the isotopic composition of the spike. Hence, improving the precision of the measured isotopic composition of the spike will improve the precision of the measured mass fractions and isotope ratio (Stracke *et al.* 2014). However, it is difficult to accurately and precisely measure the isotopic composition of the spike because of its non-natural isotopic composition, which precludes the usual internal correction for instrumental mass bias (Chu *et al.* 2011).

Due to instrumental mass bias (Albarède *et al.* 2004), measured isotope ratios must be calibrated by using rigorous mass bias correction models. Currently, the commonly used calibration methods for isotopic measurements include internal normalisation (Yang and Sturgeon 2003, Thirlwall and Anczkiewicz 2004, Nowell *et al.* 2008, Yang *et al.* 2008a), double-spike correction (Thirlwall 2000), standard–sample bracketing (SSB) (Albarède *et al.* 2004, Mason *et al.* 2004, Petit *et al.* 2008), combined standard–sample bracketing with internal standard (C-SSBIN), the regression model (White *et al.* 2000, Anbar *et al.* 2001, Willigers *et al.* 2002, Yang and Sturgeon 2009) and the full gravimetric isotope mixture model (Tong *et al.* 2019). However, for absolute isotope ratio measurements, such as the isotopic compositions of the enriched Hf spike, only the last four models can be used to correct both mass-dependent and mass-independent isotopic fractionation/mass bias (Yang *et al.* 2018). Correction of the instrumental isotopic fractionation is best achieved by the full gravimetric isotope mixture approach, which requires purely separated isotopes of all (six) Hf isotopes in weighable quantities. This approach is not feasible for Hf, especially considering the low abundance of some of its isotopes. Therefore, the cost-effective regression model for Hf isotopic ratio measurements is employed in this study. The regression model was initially proposed by Maréchal *et al.* (1999) for the determination of $^{68}Zn/^{64}Zn$, which was based on derived equations from the Russell's (mass-dependent) law. This initial regression model was later completely revised (Yang and Meija 2010) without the use of Russell's law and optimised by measuring at increments of RF power for a short measurement session (10–30 min) (Yang *et al.* 2018). Matrix separation is not strictly required as long as no significant spectroscopic interference exists on the isotopes of interest for the regression model (Zhu *et al.* 2017). Since then, the regression model has been successfully applied to the measurement of absolute isotopic compositions of many elements, for example Ir (Zhu *et al.* 2017), Os (Zhu *et al.* 2018), Sr (Yang *et al.* 2008b), Ga (Zhang *et al.* 2016) and Cu (Hou *et al.* 2015). Additionally, the optimised regression model offers a cost-effective alternative to the primary method of the full gravimetric isotope mixture model in lead isotope measurements (Tong *et al.* 2019).

To the best of our knowledge, the regression model has not been applied to the analysis of the isotopic composition of any enriched spike. The aim of this study was to extend this state-of-the-art optimised regression model to the determination of the Hf isotopic composition in an enriched spike. The IRIS-1 Ir isotope standard was used as the calibrator to obtain the mass bias-corrected $^{187}Re/^{185}Re$ ratio in the NIST SRM 3134 Re standard solution, which was then used to calibrate Hf isotope ratios in spike.

Experimental section

Reagents and reference material

Ultrapure water (18.2 MΩ cm) was acquired from a Milli-Q Element system (Millipore, Bedford, MA, USA). Commercially available nitric acid (HNO_3), hydrofluoric acid (HF) and hydrochloric acid (HCl) were further purified twice using a DST-1000 acid purification system (Savillex, Eden Prairie, MN, USA). The 2% HNO_3-0.05% HF solution consisted of concentrated HNO_3 and HF diluted with ultrapure water.

The isotopic certified reference material solution IRIS-1 (1000 µg g^{-1}) obtained from the National Research Council Canada (NRC, Ottawa, ON, Canada) with a certified value of $^{193}Ir/^{191}Ir = 1.6866 \pm 0.0005$ (u, $k = 1$) was used to calibrate $^{187}Re/^{185}Re$ in the NIST SRM 3143 Re standard solution. NIST SRM 3143 (Lot No. 010816, 10004 µg g^{-1}) solution was purchased from the National Institute of Standards and Technology, NIST, Gaithersburg, MD, USA) and was used to calibrate the $^{176}Hf/^{177}Hf$,

Table 1.
Certificate isotopic values of Hf spike

Isotope	Abundance	Certificate isotopic value ($^{x}Hf/^{177}Hf$)
^{174}Hf	0	0
^{176}Hf	0.0006	0.24
^{177}Hf	0.0025	1
^{178}Hf	0.0069	2.76
^{179}Hf	0.0072	2.88
^{180}Hf	0.9828	393.12

x = 174, 176, 177, 178, 179, 180.

$^{179}Hf/^{177}Hf$ and $^{180}Hf/^{177}Hf$ ratios. The enriched Hf spike (Oak Ridge National Laboratory, USA, Lot No. 159293, which is HfO_2 digested with concentrated HCl), was evaporated to dryness and then re-dissolved in 2% HNO_3. The certificate isotopic compositions of spike are listed in Table 1.

Instrumentation

Experiments were conducted on a Neptune *Plus* MC-ICP-MS (Thermo Fisher Scientific, Bremen, Germany) at the State Key Laboratory of Geological Processes and Mineral Resources (GPMR), China University of Geosciences, Wuhan. The instrument was equipped with nine Faraday cups, and all of the Faraday cups were equipped with 10^{11} Ω amplifier resistors. The sample solution was introduced using the standard introduction system (low-flow PFA nebuliser (~ 50 μl min^{-1}) and quartz glass spray chamber) coupled with an autosampler (ASX-112FR, Cetac Technologies, Omaha, NE, USA). The Neptune *Plus* was operated in static mode using twenty-four cycles with an integration time of 4.149 s. To improve the instrumental sensitivity, the X skimmer cone and Jet sample cone combination, as well as the guard electrode, were applied. The high field-strength elements (HFSE) generally exhibit a 'sticky' nature and easily adhered to the surfaces of the sample cone. In this study, the Hf intensity of the blank was observed to increase from 0.016 to 20 mV during analysis. The 2% HNO_3-0.05% HF was introduced for 100–120 s to reduce the memory effects of Re, Ir and Hf. With this wash, the blank intensity values of ^{193}Ir, ^{187}Re and ^{180}Hf were reduced to 0.5, 0.7 and 2 mV, respectively; even though the signal intensities for samples were as high as 25, 20 and 44 V signal intensities were still blank-corrected. Rhenium isotopes in the NIST SRM 3134 Re solution were first calibrated by the IRIS-1 Ir isotope standard by using mixed solutions of NIST SRM 3134 Re and IRIS-1, and the instrumental mass bias of the Hf isotope ratios in the spike was then calibrated by the obtained Re ratio by using the mixed solution of NIST SRM 3134 Re and Hf spike. The Faraday cup configuration and detailed operating parameters are listed in Table 2.

Sample preparation and analysis

Stock solutions of Ir, Re and Hf mentioned above were prepared by dilution with 2% HNO_3 to approximately 3–4 μg g^{-1}. For the regression correction model, the appropriate solutions (NIST SRM 3134 Re – IRIS-1 and Hf Spike – NIST SRM 3134 Re) were prepared. Detailed concentrations and signal intensities are listed in Table 3.

Recent developments in the regression model have significantly shortened the measurement time from 6–15 h to 10–30 min per session by measuring at equal increments of

Table 2.
Neptune Plus MC-ICP-MS operating conditions

Parameter	Configuration/value					
	L3	L2	C	H1	H3	H4
Cup configuration Re-Hf	^{176}Hf	^{177}Hf	^{179}Hf	^{180}Hf	^{185}Re	^{187}Re
Cup configuration Re-Ir		^{185}Re	^{187}Re	^{191}Ir	^{193}Ir	
Mass dispersion	17%					
RF power	1204 W					
Plasma gas flow	16.0 l min^{-1}					
Auxiliary gas flow	0.71 l min^{-1}					
Sample gas flow	0.694 l min^{-1}					
Interface cones	Jet sample cone + X skimmer cone					
Guard electrode (GE)	On					
Block × cycle	6 × 4					
Integration time	4.194 s					

Table 3.
The mass fractions and signal intensities of sample and calibrator

Sample	Mass fr. ($\mu g\ g^{-1}$)	Intensity (V)	Calibrator	Mass fr. ($\mu g\ g^{-1}$)	Intensity (V)
NIST SRM 3134 Re	3.5	^{187}Re: 25	IRIS-1	3	^{193}Ir: 20
Spike Hf	~ 4.0	^{180}Hf: 46	NIST SRM 3134 Re	3.5	^{187}Re: 25

Enriched Hf spike was purchased from Oak Ridge National Laboratory, USA (Lot No. 159293).

plasma RF power (Heidenreich and Thiemens 1983, Zhu *et al.* 2017), thus making the optimised regression model (ORM) suitable for applications requiring small sample sizes. In this study, we adopted this ORM model by measuring isotope ratios at equal increments from the RF P_0 (highest sensitivity and stable signal) to P_{max}, whereas the sensitivity decreases by 25% compared with P_0. A session of measurements consisting of four points with equal increments of $P = (P_{max} - P_0) \cdot N/3$, where $N = 0$, 1, 2, and 3 ($P_0 < P_1 < P_2 < P_{max}$), and one blank measurement at P_0 requires approximately 15 min. The signals of the 2% HNO_3-0.05% HF blank at P_0, were subtracted from all samples.

Results and discussion

Correction for instrumental mass bias

This regression model is based on the observed correlated temporal drift between isotope ratios of analyte and calibrator, a linear relationship between $\ln r^{analyte}$ and $\ln r^{calibrant}$. Although identical mass bias between the analyte and calibrator is not required in the regression model method, it was found that better precision with respect to isotope ratio was obtained when the mass of the calibrator is similar to that of the analyte (Hou *et al.* 2015). In theory, the Hf isotope ratios can be calibrated by the Re isotope ratio, and the isotopes of the two elements can be measured in a static run for the best results. Unfortunately, the NIST SRM 989 Re isotope standard was out of stock, and there was no other Re isotope certified reference material available.

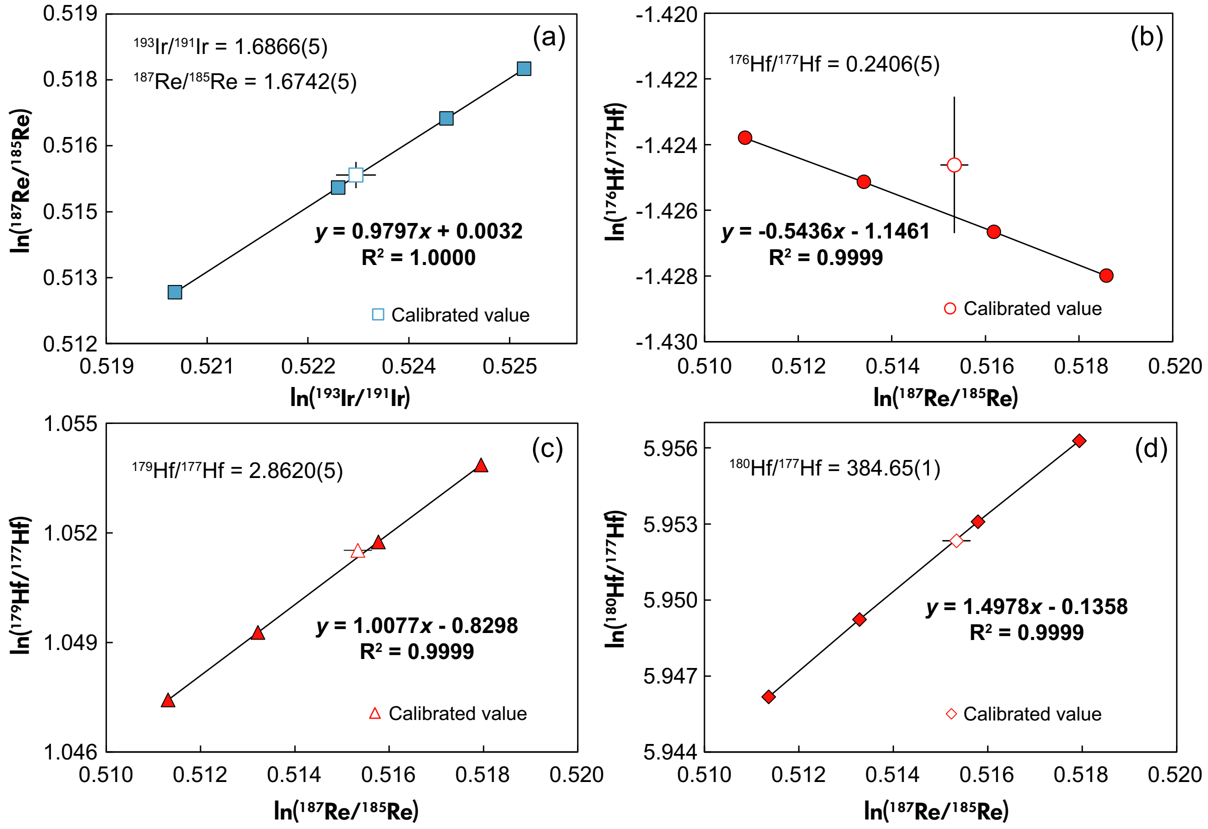

Figure 1. The measured isotopic ratio regressions of Ir-Re solution (a) in (IRIS-1 + NIST SRM 3134 Re) solution, Re-Hf (b–d) in (spike Hf + NIST SRM 3134 Re) solution.

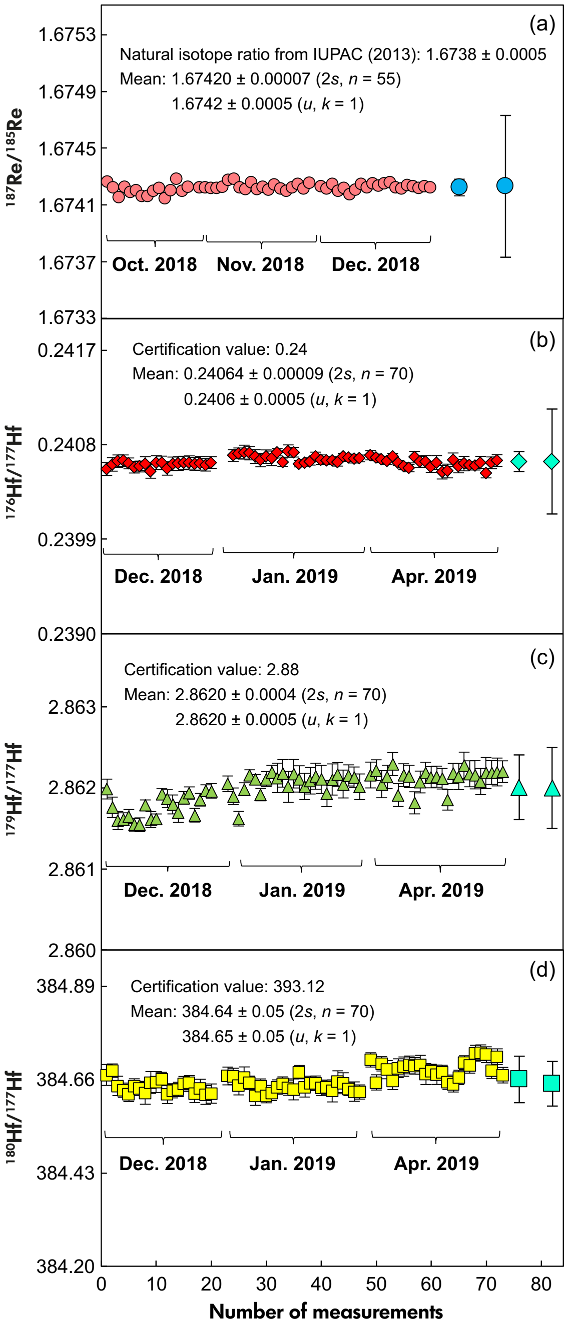

Figure 2. Calibrated Hf isotopic ratios in the Hf spike obtained by the regression model. The error of the analytical data calibrated by the three methods is 2*s*, and the combined uncertainty (*u*, *k* = 1) of the data calibrated by the regression model is also shown.

Consequently, the IRIS-1 Ir isotope standard was used to calibrate the ^{187}Re/^{185}Re ratio in NIST SRM 3134 (Re standard solution) by the optimised regression model. The Hf isotope ratios of the enriched spike in the NIST SRM 3134 Re solution could then be accurately measured with the calibrated ^{187}Re/^{185}Re value.

The regression models of Re-Ir and Hf-Re can be expressed by Equations (1, 2) in accordance with Zhu *et al.* (2017) and Yang (2009):

$$\ln(r^{Re}_{187/185}) = a_1 + b_1 \cdot \ln(r^{Ir}_{193/191})$$

$$\ln(r^{Hf}_{i/177}) = a_2 + b_2 \cdot \ln(r^{Re}_{187/185}) \qquad (1)$$

where coefficients *a* and *b* are the intercept and slope of the corresponding linear regression that are obtained using least squares fitting of data, and i = 176, 179 and 180. Here, the true isotope ratio (R) is directly linked to its measured ratio by a correction factor K: $R^{Re}_{187/185} = K^{Re}_{187/185} \cdot r^{Re}_{187/185}$, $R^{Ir}_{193/191} = K^{Ir}_{193/191} \cdot r^{Ir}_{193/191}$ and $R^{Hf}_{i/177} = K^{Hf}_{i/177} \cdot r^{Hf}_{176/177}$. Together, the above equations produce the measurement model for the calibrated isotope ratios, which are free from untested assumptions of identical isotopic fractionation for different isotope pairs (Gall *et al.* 2012):

$$R^{Re}_{187/185} = e^{a_1} \cdot (R^{Ir}_{193/191})^{b_1}$$

$$R^{Hf}_{176/177} = e^{a_2} \cdot (R^{Re}_{187/185})^{b_2} \qquad (2)$$

It is important to note that Equation (2) is not derived from either the exponential law or Russell's law and is able to calibrate both mass-dependent and mass-independent fractionation occurring in MC-ICP-MS (Yang *et al.* 2018). This condition induces an adequate temporal mass bias drift to form a good linear relationship between ln(^{193}Ir/^{191}Ir)-ln(^{187}Re/^{185}Re) or ln(^{187}Re/^{185}Re)-ln(^{176}Hf/^{177}Hf), ln(^{179}Hf/^{177}Hf) and ln(^{180}Hf/^{177}Hf) while maintaining suitable sensitivity for the observed isotope signals.

Measurement results of Re and Hf isotope ratios

Fifty-five sets of ln(^{193}Ir/^{191}Ir)-ln(^{187}Re/^{185}Re) data and seventy sets of ln(^{187}Re/^{185}Re)-ln(^{176}Hf/^{177}Hf) data were acquired in Ir-Re and Re-Hf solutions over a five-month period. The relationships of ln(^{193}Ir/^{191}Ir)-ln(^{187}Re/^{185}Re) and ln(^{187}Re/^{185}Re)-ln(^{176}Hf/^{177}Hf), ln(^{179}Hf/^{177}Hf) and ln(^{180}Hf/^{177}Hf) were linearly correlated and exhibited high correlation coefficients ($R^2 > 0.9995$) (Figure 1). With the good linear correlation between ln(^{193}Ir/^{191}Ir) and ln(^{187}Re/^{185}Re), a value of ^{187}Re/^{185}Re = 1.6742 ± 0.0005 (*u*, *k* = 1) in NIST SRM 3134 Re was accurately calculated by Equation (2), which can be used to calculate

Table 4.
Calibrated Re and Hf isotope ratios in NIST 3134 Re and enriched Hf spike using the regression model

Sample	Calibrator	Batch	Isotopic ratio	Combined uncert ^{a}	*N*	Date
NIST 3134 Re	IRIS-1	**^{187}Re/^{185}Re**				
		Batch 1	1.6742	0.0005	15	Oct. 2018
		Batch 2	1.6742	0.0005	20	Nov. 2018
		Batch 3	1.6742	0.0005	20	Dec. 2018
		Combined value	1.6742	0.0005	55	
		RV	–			
Spike	NIST 3134 Re	**^{176}Hf/^{177}Hf**				
		Batch 1	0.2406	0.0005	20	Dec. 2018
		Batch 2	0.2407	0.0005	25	Jan. 2019
		Batch 3	0.2406	0.0005	25	Apr. 2019
		Combined value	0.2406	0.0005	70	
		Certificate value	0.24			
		^{179}Hf/^{177}Hf				
		Batch 1	2.8618	0.0005	20	Dec. 2018
		Batch 2	2.8620	0.0005	25	Jan. 2019
		Batch 3	2.8621	0.0005	25	Apr. 2019
		Combined value	2.8620	0.0005	70	
		Certificate value	2.88			
		^{180}Hf/^{177}Hf				
		Batch 1	384.64	0.03	20	Dec. 2018
		Batch 2	384.64	0.06	25	Jan. 2019
		Batch 3	384.67	0.06	25	Apr. 2019
		Combined value	384.65	0.05	70	
		Certificate value	393.12			

RV, recommended value.

[a] The combined uncertainty (u, $k = 1$), which includes all uncertainty contributions from the measurement process.

the Hf isotope ratios in the Hf spike. The measured value of ^{187}Re/^{185}Re = 1.6742(5)$_{k=1}$ in NIST SRM 3134 Re was in good agreement with the value adopted by IUPAC [^{187}Re/^{185}Re = 1.6739 ± 0.0010 (Gramlich *et al.* 1973), 1.6738 ± 0.0005 (Meija *et al.* 2016), 1.6737 ± 0.0002 (Berglund and Wieser 2011) and 1.6738 ± 0.0002 (De Laeter *et al.* 2003)] within error. Over the 5-month period, the obtained Hf isotope ratios exhibited little variation, even with different daily optimisation conditions (Figure 2), demonstrating the robustness of the regression model. The obtained final values of ^{176}Hf/^{177}Hf, ^{179}Hf/^{177}Hf and ^{180}Hf/^{177}Hf in the Hf spike were 0.2406 ± 0.0005 (u, $k = 1$), 2.8620 ± 0.0005 (u, $k = 1$) and 384.65 ± 0.05 (u, $k = 1$), respectively (Table 4), meeting the required precision level for applying the ID method. The reported combined uncertainties include all uncertainty contributions from the measurement of the Re and Hf isotope ratios evaluated using a Monte Carlo method, in which the uncertainty of the primary calibrator (IRIS-1, ^{193}Ir/^{191}Ir = 1.6866 ± 0.0005, u, $k = 1$) was also taken into consideration.

Comparison of the regression method with the SSB and C-SSBIN methods

Instrumental mass bias is typically corrected using either the SSB or the C-SSBIN methods. To highlight the accurate and precise results obtained by the regression model, the SSB and C-SSBIN methods were also applied to measure the Hf isotope ratios of the enriched spike (Figure 3 , Tables S1, S2 and S3).

The values of ^{176}Hf/^{177}Hf, ^{179}Hf/^{177}Hf and ^{180}Hf/^{177}Hf calibrated by SSB were 0.240 ± 0.003 (2*s*, $n = 20$), 2.90 ± 0.15 (2*s*, $n = 20$) and 391 ± 27 (2*s*, $n = 20$), respectively. These obtained precisions do not meet the requirement for the application of the ID method. The C-SSBIN method can produce more accurate and precise isotope ratios, whereby an internal standard element was added to both the sample and calibrator (Yang *et al.* 2008b). Close matching of mass fractions of both the analyte and internal standard element in the sample and standard is also required. In this study, the diluted NIST SRM

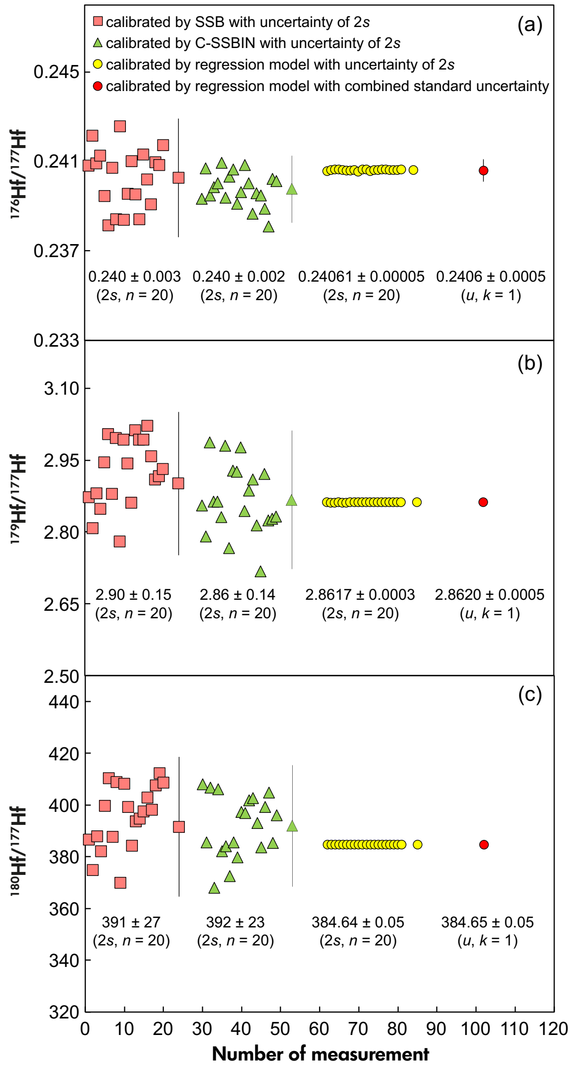

Figure 3. ^{176}Hf/^{177}Hf, ^{179}Hf/^{177}Hf and ^{180}Hf/^{177}Hf ratios of the enriched Hf spike calibrated by SSB, C-SSBIN and regression model methods. The reported error of the analytical data is 2*s*. The combined uncertainty (*u*, *k* = 1) of the data calibrated by the regression model is also shown.

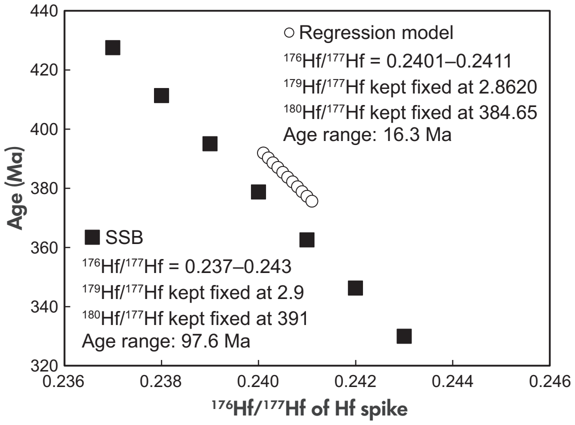

Figure 4. The deviation in calculated isochron ages between the precision of spike Hf when using the ratios determined by the SSB method and the regression model method.

3143 Re (3 µg g^{-1}) was used as the internal standard added to the enriched Hf spike (approximately 3 µg g^{-1}) and alfa Hf (3 µg g^{-1}). The obtained ^{176}Hf/^{177}Hf, ^{179}Hf/^{177}Hf and ^{180}Hf/^{177}Hf values using the C-SSBIN method were 0.240 ± 0.002 (2*s*, *n* = 20), 2.86 ± 0.14 (2*s*, *n* = 20) and 392 ± 23 (2*s*, *n* = 20). While the precision was improved compared with the SSB method, the obtained precisions do meet the requirements for application of the ID method. Using the regression model method, the obtained Hf isotopic ratios were ^{176}Hf/^{177}Hf = 0.24061 ± 0.00005 (2*s*, *n* = 20), ^{179}Hf/^{177}Hf = 2.8617 ± 0.0003 (2*s*, *n* = 20) and ^{180}Hf/^{177}Hf = 384.64 ± 0.03 (2*s*, *n* = 20), respectively. The uncertainties were also estimated as the combined uncertainties (*u*, *k* = 1), which included all uncertainty contributions from the measurement process using the Monte Carlo method with proper accounting for the uncertainty due to the primary calibrator (IRIS-1, ^{193}Ir/^{191}Ir = 1.6866 ± 0.0005, *u*, *k* = 1), also shown in Figure 3. Thus, the precision obtained using the regression model was significantly better than the precisions obtained by either the SSB or C-SSBIN methods, and not as dependent on matrix matching.

Effect of the precision in isotopic composition spike Hf on calculated isochron age

In the application of the ID method, the accurate and precise measurement of elemental mass fraction is affected by the spike calibration uncertainty (Stracke *et al.* 2014), which, in turn, affect the calculated isochron age (Blichert-Toft *et al.* 1997, Weyer *et al.* 2002). The precision of the isotopic composition in the enriched Hf spike was significantly improved by the regression model. For example, the stated uncertainty of the ^{180}Hf/^{177}Hf ratio was a factor of ten better compared with that provided by Weyer *et al.* (2002). To investigate the effect of the increase in precision on the calculation of the Lu-Hf isochron age, the isochron age was calculated using SSB and regression model data for the enriched Hf spike (Figure 4). Three isotopic ratios (^{176}Hf/^{177}Hf, ^{179}Hf/^{177}Hf and ^{180}Hf/^{177}Hf) of the Hf spike are needed to calculate isochron age. To investigate the effect of the precision in isotopic composition of the enriched Hf spike on the calculated isochron age, the precision of the ^{176}Hf/^{177}Hf ratio was varied, while the precision of

^{179}Hf/^{177}Hf and ^{180}Hf/^{177}Hf ratios was kept constant (Figure 4). When the ratios determined by the SSB method were used (^{176}Hf/^{177}Hf = 0.237–0.243 and ^{179}Hf/^{177}Hf and ^{180}Hf/^{177}Hf were 2.90 and 391), there was a potential ~ 97.6 Ma offset of the calculated isochron age (Figure 4). When the ratios determined using the regression model method (^{176}Hf/^{177}Hf = 0.2401–0.2411, ^{179}Hf/^{177}Hf and ^{180}Hf/^{177}Hf were 2.8620 and 384.65) were used, the offset was only ~ 16 Ma. Therefore, the application of the newly calibrated enriched Hf spike should significantly reduce the uncertainty of measuring the mass fraction of Hf and increase the accuracy of the Lu-Hf chronometer.

Conclusions

A regression model was successfully applied to the determination of the isotopic composition of an enriched Hf spike for the first time. The obtained Hf isotope ratios (^{176}Hf/^{177}Hf, ^{179}Hf/^{177}Hf and ^{180}Hf/^{177}Hf) were 0.2406 ± 0.0005 (u, k = 1), 2.8620 ± 0.0005 (u, k = 1) and 384.65 ± 0.05 (u, k = 1), respectively. The obtained precision of ^{176}Hf/^{177}Hf, ^{179}Hf/^{177}Hf and ^{180}Hf/^{177}Hf was improved significantly compared with both the SSB and C-SSBIN methods. Using the isotope ratio determined with the regression model, the offset of the calculated isochron age was improved to ~ 16 Ma, compared with ~ 97.6 Ma using data from the SSB method. Thus, with the application of the regression model, the calculated isochron Lu-Hf age was significantly improved. In addition to the above advantages, the regression method can address both mass-dependent and mass-independent fractionation in MC-ICP-MS. Thus, it can be applied in the future to calibrate the isotopic composition of other enriched isotopic spikes.

Acknowledgements

This work was funded by the National Natural Science Foundation of China (41803015 and 41922021), the 111 Project (BP0719022), the MOST Special Funds of the State Key Laboratory of Geological Processes and Mineral Resources (MSFGPMR01), the National Key R&D Program of China (2016YFC0600103) and the National Program on Key Basic Research Project (2015CB856101).

References

Albarède F., Télouk P., Blichert-Toft J., Boyet M., Agranier A. and Nelson B. (2004)
Precise and accurate isotopic measurements using multiple-collector ICP-MS. Geochimica et Cosmochimica Acta, 68, 2725–2744.

Anbar A., Knab K. and Barling J. (2001)
Precise determination of mass-dependent variations in the isotopic composition of molybdenum using MC-ICP-MS. Analytical Chemistry, 73, 1425–1431.

Barfod G.H., Otero O. and Albarède F. (2003)
Phosphate Lu-Hf geochronology. Chemical Geology, 200, 241–253.

Blichert-Toft J., Chauvel C. and Albarède F. (1997)
Separation of Hf and Lu for high-precision isotope analysis of rock samples by magnetic sector-multiple collector ICP-MS. Contributions to Mineralogy and Petrology, 127, 248–260.

Blichert-Toft J. (2001)
On the Lu-Hf isotope geochemistry of silicate rocks. Geostandards Newsletter: The Journal of Geostandards and Geoanalysis, 25, 41–56.

Becker J.S. and Dietze H.-J. (1998)
Inorganic trace analysis by mass spectrometry. Spectrochimica Acta Part B, 53, 1475–1506.

Beranoaguirre A., Pin C., Sanchez-Lorda M.E., De Madinabeitia S.G. and Gil Ibarguchi J.I. (2019)
An evaluation of Rb-Sr isotope dilution analyses with a ^{86}Sr-enriched tracer and multiple collection-ICP-MS. International Journal of Mass Spectrometry, 435, 234–240.

Brun V., Masselon C., Garin J. and Dupuis A. (2009)
Isotope dilution strategies for absolute quantitative proteomics. Journal of Proteomics, 72, 740–749.

Berglund M. and Wieser M.E. (2011)
Isotopic compositions of the elements 2009 (IUPAC Technical Report). Pure and Applied Chemistry, 83, 397–410.

Cheng H., Zhang C., Vervoort J.D., Li X., Li Q., Wu Y. and Zheng S. (2012)
Timing of eclogite facies metamorphism in the North Qinling by U-Pb and Lu–Hf geochronology. Lithos, 136–139, 46–59.

Chu Z., Yang Y., Jinghui G. and Qiao G. (2011)
Calculation methods for direct internal mass fractionation correction of spiked isotopic ratios from multi-collector mass spectrometric measurements. International Journal of Mass Spectrometry, 299, 87–93.

De Laeter J.R., Böhlke J.K., De Bièvre P., Hidaka H., Peiser H., Rosman K. and Taylor P. (2003)
Atomic weights of the elements. Review 2000 (IUPAC Technical Report). Pure and Applied Chemistry, 75, 683–800.

Gopalan K. (2011)
High precision isotope dilution determination of potassium by thermal ionisation mass spectrometry. Geostandards and Geoanalytical Research, 35, 175–181.

Gall L., Williams H., Siebert C. and Halliday A. (2012)
Determination of mass-dependent variations in nickel isotope compositions using double spiking and MC-ICP-MS. Journal of Analytical Atomic Spectrometry, 27, 137–145.

references

Gramlich J.W., Murphy T.J., Garner E.L. and Shields W.R. (1973)
Absolute isotopic abundance ratio and atomic weight of a reference sample of rhenium. Journal of Research of the National Bureau of Standards, 77, 691–698.

Herwartz D., Nagel T.J., Münker C., Scherer E.E. and Froitzheim N. (2011)
Tracing two orogenic cycles in one eclogite sample by Lu-Hf garnet chronometry. Nature Geoscience, 4, 178–183.

Hou Q.H., Zhou L., Gao S., Zhang T., Feng L. and Yang L. (2015)
Use of Ga for mass bias correction for the accurate determination of copper isotope ratio in the NIST SRM 3114 Cu standard and geological samples by MC-ICP-MS. Journal of Analytical Atomic Spectrometry, 31, 280–287.

Heidenreich J.E. III and Thiemens M.H. (1983)
A non-mass-dependent isotope effect in the production of ozone from molecular oxygen. The Journal of Chemical Physics, 78, 892–895.

Lagos M., Scherer E.E., Tomaschek F., Münker C., Keiter M., Berndt J. and Ballhaus C. (2007)
High precision Lu–Hf geochronology of Eocene eclogite-facies rocks from Syros, Cyclades, Greece. Chemical Geology, 243, 16–35.

Le Fèvre B. and Pin C. (2005)
A straightforward separation scheme for concomitant Lu–Hf and Sm–Nd isotope ratio and isotope dilution analysis. Analytica Chimica Acta, 543, 209–221.

Marshall R. and Hess D. (1960)
Determination of very small quantities of lead. Analytical Chemistry, 32, 960–966.

Mason T.F.D., Weiss D.J., Horstwood M., Parrish R.R., Russell S.S., Mullane E. and Coles B.J. (2004)
High-precision Cu and Zn isotope analysis by plasma source mass spectrometry. Journal of Analytical Atomic Spectrometry, 19, 209–217.

Maréchal C.N., Télouk P. and Albarède F. (1999)
Precise analysis of copper and zinc isotopic compositions by plasma-source mass spectrometry. Chemical Geology, 156, 251–273.

Meija J., Coplen T.B., Berglund M., Brand W.A., De Bièvre P., Gröning M., Holden N.E., Irrgeher J., Loss R.D. and Walczyk T. (2016)
Isotopic compositions of the elements 2013 (IUPAC technical Report). Pure and Applied Chemistry, 88, 293–306.

Nowell G.M., Luguet A., Pearson D.G. and Horstwood M.S.A. (2008)
Precise and accurate ^{186}Os/^{188}Os and ^{187}Os/^{188}Os measurements by multi-collector plasma ionisation mass spectrometry (MC-ICP-MS) part I: Solution analyses. Chemical Geology, 248, 363–393.

Patchett P. and Tatsumoto M. (1980a)
Hafnium isotope variations in oceanic basalts. Geophysical Research Letters, 7, 1077–1080.

Patchett P. and Tatsumoto M. (1980b)
Lu–Hf total-rock isochron for the eucrite meteorites. Nature, 288, 571–574.

Petit J., De Jong J., Chou L. and Mattielli N. (2008)
Development of Cu and Zn isotope MC-ICP-MS measurements: Application to suspended particulate matter and sediments from the Scheldt Estuary. Geostandards and Geoanalytical Research, 32, 149–166.

Scherer E., Münker C. and Mezger K. (2001)
Calibration of the lutetium-hafnium clock. Science, 293, 683–687.

Scherer E.E., Cameron K.L. and Blichert-Toft J. (2000)
Lu–Hf garnet geochronology: Closure temperature relative to the Sm–Nd system and the effects of trace mineral inclusions. Geochimica et Cosmochimica Acta, 64, 3413–3432.

Smit M.A., Scherer E.E. and Mezger K. (2013)
Lu–Hf and Sm–Nd garnet geochronology: Chronometric closure and implications for dating petrological processes. Earth and Planetary Science Letters, 381, 222–233.

Shu Q., Brey G.P., Gerdes A. and Hoefer H.E. (2014)
Mantle eclogites and garnet pyroxenites – The meaning of two-point isochrons, Sm–Nd and Lu–Hf closure temperatures and the cooling of the subcratonic mantle. Earth and Planetary Science Letters, 389, 143–154.

Stracke A., Scherer E.E. and Reynolds B.C. (2014)
Application of isotope dilution in geochemistry. Treatise on Geochemistry, 71–86.

Thirlwall M.F. and Anczkiewicz R. (2004)
Multidynamic isotope ratio analysis using MC–ICP–MS and the causes of secular drift in Hf, Nd and Pb isotope ratios. International Journal of Mass Spectrometry, 235, 59–81.

Thirlwall M.F. (2000)
Inter-laboratory and other errors in Pb isotope analyses investigated using a ^{207}Pb–^{204}Pb double spike. Chemical Geology, 163, 299–322.

Tong S., Meija J., Zhou L., Methven B., Mester Z. and Yang L. (2019)
High-precision measurements of the isotopic composition of common lead using MC-ICP-MS: Comparison of calibration strategies based on full gravimetric isotope mixture and regression models. Analytical Chemistry, 6, 4164–4171.

Waight T., Baker J. and Willigers B. (2002)
Rb isotope dilution analyses by MC-ICP-MS using Zr to correct for mass fractionation: Towards improved Rb–Sr geochronology? Chemical Geology, 186, 99–116.

references

Willbold M. and Jochum K.P. (2010)
Multi-element isotope dilution sector field ICP-MS: A precise technique for the analysis of geological materials and its application to geological reference materials. Geostandards and Geoanalytical Research, 29, 63–82.

White W.M., Albarède F. and Télouk P. (2000)
High-precision analysis of Pb isotope ratios by multi-collector ICP-MS. Chemical Geology, 167, 257–270.

Willigers B., Baker J., Krogstad E. and Peate D. (2002)
Precise and accurate *in situ* Pb-Pb dating of apatite, monazite, and sphene by laser ablation multiple-collector ICP-MS. Geochimica et Cosmochimica Acta, 66, 1051–1066.

Weyer S., Münker C., Rehkämper M. and Mezger K.J.C.G. (2002)
Determination of ultra-low Nb, Ta, Zr and Hf concentrations and the chondritic Zr/Hf and Nb/Ta ratios by isotope dilution analyses with multiple collector ICP-MS. Chemical Geology, 187, 295–313.

Yang L. and Sturgeon R. (2003)
Comparison of mass bias correction models for the examination of isotopic composition of mercury using sector field ICP-MS. Journal of Analytical Atomic Spectrometry, 18, 1452–1457.

Yang Y., Zhang H., Xie L. and Wu F. (2008a)
Accurate measurement of neodymium isotopic composition using Neptune MC-ICP-MS. Frontiers of Chemistry in China, 3, 94–98.

Yang L. and Sturgeon R.E. (2009)
Isotopic fractionation of mercury induced by reduction and ethylation. Analytical and Bioanalytical Chemistry, 393, 377–385.

Yang L., Tong S., Zhou L., Hu Z., Mester Z. and Meija J. (2018)
A critical review on isotopic fractionation correction methods for accurate isotope amount ratio measurements by MC-ICP-MS. Journal of Analytical Atomic Spectrometry, 33, 1849–1861.

Yang L. and Meija J. (2010)
Resolving the germanium atomic weight disparity using multicollector ICP-MS. Analytical Chemistry, 82, 4188–4193.

Yang L., Peter C., Panne U. and Sturgeon R.E. (2008b)
Use of Zr for mass bias correction in strontium isotope ratio determinations using MC-ICP-MS. Journal of Analytical Atomic Spectrometry, 23, 1269–1274.

Yang L. (2009)
Accurate and precise determination of isotopic ratios by MC-ICP-MS: A review. Mass Spectrometry Reviews, 28, 990–1011.

Zhu Z., Meija J., Zheng A., Mester Z. and Yang L. (2017)
Determination of the isotopic composition of iridium using multicollector-ICP-MS. Analytical Chemistry, 89, 9375–9382.

Zhu Z., Meija J., Tong S., Zheng A., Zhou L. and Yang L. (2018)
Determination of the isotopic composition of osmium using MC-ICP-MS. Analytical Chemistry, 90, 9281–9288.

Zhang T., Zhou L., Yang L., Wang Q., Feng L.P. and Liu Y.S. (2016)
High precision measurements of gallium isotopic compositions in geological materials by MC-ICP-MS. Journal of Analytical Atomic Spectrometry, 31, 1673–1679.

Supporting information

The following supporting information may be found in the online version of this article:

Table S1. Measurement results for ^{176}Hf/^{177}Hf, ^{179}Hf/^{177}Hf and ^{180}Hf/^{177}Hf in the Hf spike obtained by SSB.

Table S2. Measurement results for ^{176}Hf/^{177}Hf, ^{179}Hf/^{177}Hf and ^{180}Hf/^{177}Hf in the Hf spike obtained by C-SSBIN.

Table S3. Measurement results for ^{176}Hf/^{177}Hf, ^{179}Hf/^{177}Hf and ^{180}Hf/^{177}Hf in the Hf spike obtained by the regression model method.

This material is available from: http://onlinelibrary.wiley.com/doi/10.1111/ggr.12343/abstract (This link will take you to the article abstract).